



Optimization of a 27 MHz Wireless Power Transmitter for Unknown Receiver

Ghulam Murtaza⁽¹⁾, Mazen Shanawani⁽¹⁾, Diego Masotti⁽¹⁾, and Alessandra Costanzo⁽¹⁾

(1) Dept. of Electrical, Electronic and Information Engineering "Guglielmo Marconi", University of Bologna, Italy

Abstract

This work describes the design of a WPT transmitter connected to a planar coil, designed by EM simulation, for the near-field wireless power transfer (WPT) of 25 W at 27 MHz to an almost unknown receiving section. A class-E inverter in GaN technology has been adopted to achieve constant current condition and high performance for its load-independent operation. A careful control of the overall efficiency of the WPT systems is provided during the different steps of the optimization process. The manuscript highlights the importance of the realistic description of both the amplifier and the loop for the sake of the project reliability.

1 Introduction

As the wireless power transfer is getting more and more important, the need for higher efficiencies is also increasing. Hence, in the recent years there is a significant increase in the utilization of the switching inverters as transmitters, because of their higher efficiency [1] [2]. However, achieving higher efficiencies is not easy for switching inverters, as well. One of the problems in that regard is the switching losses at higher frequencies. To overcome these limitations the important concept of *soft switching* has been introduced [3]. In addition to the switching losses, parasitic losses both in the coils and circuit lumped elements are further reasons for the efficiency degradation.

The object of this work is investigate the conditions to provide constant power with variable transmitter loads without significant degradation of the efficiency. For this purpose, different strategies are available in the literature to mitigate the load variation, such as ensuring constant coupling between the transmitter and the receiver [4] [5]. Similarly, utilization of a varactor is also discussed in [6] to compensate the effect of load variations. The solution adopted in this work is twofold: i) to carry on a Class E switching amplifier design to guarantee constant inverter current to an almost unknown receivers, ii) to utilize a GaN (GS66508b) device as a switch because of its wideband gap property which enables it to work on higher switching frequencies and to minimize the losses [7].

2 Class E Inverter

Conventional power converters are considered to be load independent, but majority of them are designed for 50Ω load, working at kHz frequency ranges, and utilizing *hard*

switching [8], which means that the losses in the switch are significant because the condition of having either switch voltage or switch current equal to zero at any instant is not satisfied. Whereas Class E amplifiers are also considered load independent, and able to reach MHz frequency ranges with minimum switching losses. These losses are reduced by the zero-voltage switching (ZVS) and zero-derivative switching (ZDS) conditions. These two properties are also referred to as *soft switching* in the literature [3]. These properties are simply given by:

$$V_s(\omega t) = 0. \quad (1)$$

$$\frac{dV_s(\omega t)}{d\omega t} = 0. \quad (2)$$

Where V_s is the output switch voltage. In (2) the derivative of the switch voltage should be zero at $\omega t = 2\pi$. A detailed mathematical derivation of them is given in [3].

If both of these conditions are satisfied, then the inverter is considered to be working in the optimum condition. The optimum condition is difficult to achieve being of course dependent upon many factors such as switching frequency, duty cycle of the wave driving the switch, and the load.

3 Optimization of the Class E inverter

As mentioned before, class E inverters can be designed for a certain load and frequency; in the present design we do not consider a specific load condition, being our link not a predetermined one. The design constraints are i) a power at 27 MHz delivered to the transmitting coil around 25 W, ii) a receiving coil of unknown shape, but resonating at 27 MHz, and iii) a link distance ranging from 20 to 40 cm. In our design we decided to refer to a $R_L = 120\Omega$ load loading the receiving coil, representing a quite typical input resistance of common receivers. We also chose a 50 % duty cycle of the switching waveform driving the gate of the GaN device: the input waveform shape is an additional design parameter at the designer's disposal, having a big impact on the output switch voltage, hence on the inverter efficiency. The 50% duty cycle here adopted is suggested in [3], because of the higher power output capability.

Fig. 1 shows the scheme of the proposed inverter, where a reactive network is also placed before the transmitting loop while keeping the receiving part almost unknown.

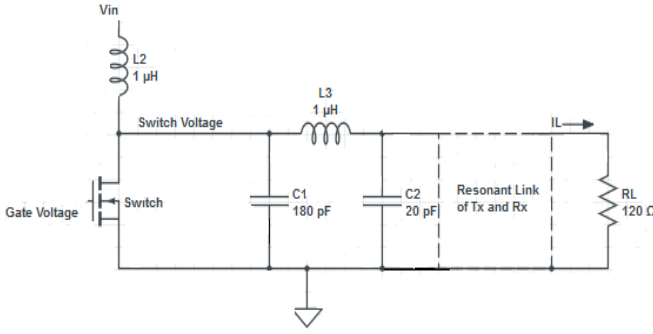


Figure 1. Schematic of the WPT link circuit.

In Fig. 1, the shunt capacitor C_1 is responsible for the shaping of the switch voltage and it also filters out the higher harmonics.

The reactive inverter output network consists of a shunt capacitance (C_2) and a series inductance (L_3): as previously said, it allows to drive the inverter under optimum condition for 120Ω load at the receiver side. We rely on the Class E capability of load-independency to manage different loading conditions, in order to emulate the situation of unknown receiver characteristics. The input drain dc voltage is chosen to be 8.5 V, whereas a square waveform at 27MHz is applied at the gate terminal which fluctuates between 0V-5V with 50% duty cycle.

As a first trial to test the GaN device, a T network has been chosen to represent the inductive link between transmitter and receiver (see Fig. 2).

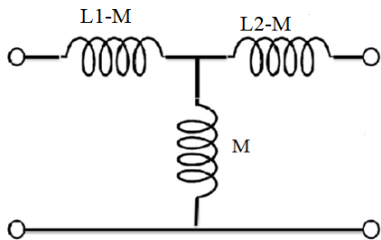


Figure 2. Inductive link between Tx and Rx equivalent representation.

L_1 represents the inductance of the transmitting coil and is chosen equal to $1 \mu\text{H}$, whereas L_2 is the unknown inductance of the receiving coil, considered equal to 500 nH . M equal to 70 nH is the mutual inductance, evaluated in order to have a 0.1 coupling coefficient (k).

A nonlinear optimization with C_1 , C_2 and L_3 as design parameters is carried out. Fig. 3 shows the output drain voltage of the switch obtained for $C_1=180 \text{ pF}$, $C_2=20 \text{ pF}$, $L_3=10 \text{ nH}$: it can be seen that the voltage across the switch is in the optimum operating conditions providing zero voltage and zero derivative conditions.

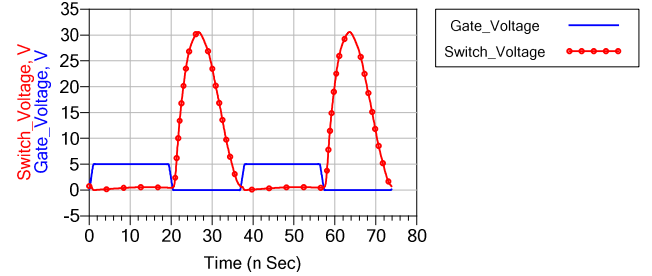


Figure 3. Gate and switch voltages for $k= 0.1$.

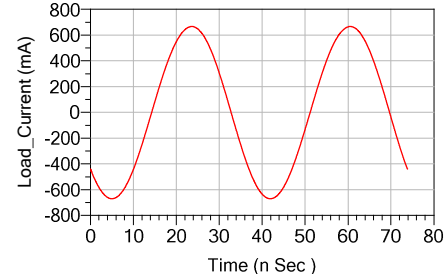


Figure 4. Current waveform on the load R_L for $k= 0.1$

The current waveform on the inverter output, shown in Fig. 4, is sinusoidal which indicates that all the higher harmonics have been properly suppressed. Overall power added efficiency of the system in this case is 78%. Spice models for all the components have been used to make the simulations more accurate: in this first design stage the two coils (L_1 and L_2) are considered ideal, at this stage.

One of the major sources of the losses in the switching amplifier is the switch itself. When an ideal switch is considered, the class E switching amplifier has the ability to deliver power with more than 90% of efficiency.

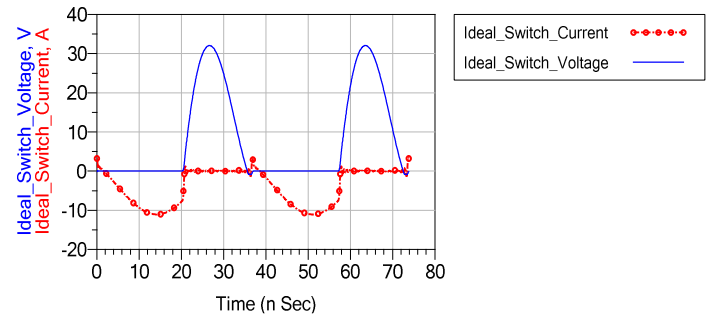


Figure 5. Ideal switch waveforms

In Fig. 5, where the current and voltage waveforms of an ideal switch are reported, it can be seen that the product of current through the ideal switch and the voltage across it, is almost zero at every instant, thus leading to very low power losses in this case.

However, in case of the GaN (GS66508b) switch in Fig. 6 it can be observed that the product of current and voltage is not always zero and, as a consequence, the efficiency is reduced to 78%, in our case.

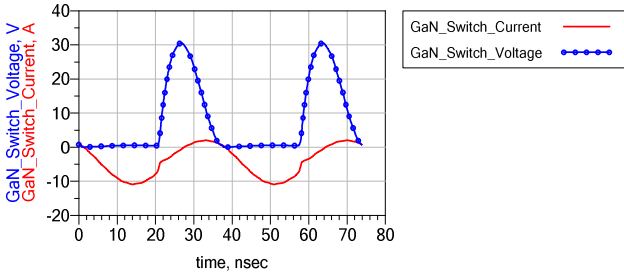


Figure 6. GaN Switch waveforms

Another parameter which strongly affects the link efficiency are the parasitic losses of the coils. Higher parasitic losses reduce the efficiency of the inverter significantly, as discussed later.

Moreover, in order to check the behavior of the transmitter when changing the link conditions, the load has been varied from 100Ω to 140Ω and the corresponding switch voltage and current waveforms are given in Fig. 7.

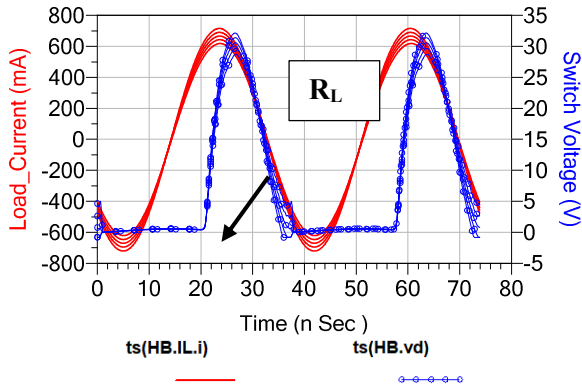


Figure 7. Switch voltage for load variation.

We can see that, as the load varies, there is a small degradation in the shape of the switch voltage and the variation in current is very small as well: the corresponding efficiency values ranges from 75% to 80%. However, when the real part of the transmitting loop impedance is increased from $0\ \Omega$ (as the ideal case considered before) to $0.36\ \Omega$, the efficiency of the link decreases: if we consider again the case of $R_L=120\Omega$, it varies from 78% to 62%, which is a considerable loss in the efficiency.

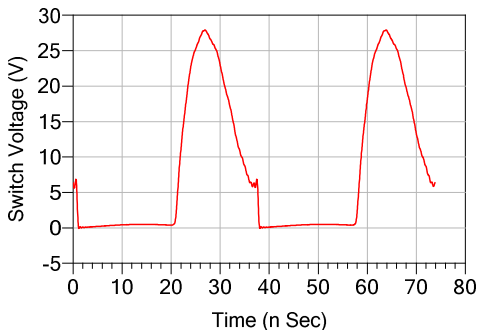


Figure 8 Switch voltage for the lossy coil

It is evident from Fig. 8 that part of the efficiency loss is because of the degradation of the switch voltage waveform,

which deviates from its optimum shape because of the parasitic losses in the antenna.

4 Realistic wireless link design

A realistic link between the transmitter coil and a generic receiver has been designed and electromagnetically simulated. Fig. 9 shows the link under examination, where both the coils have a protective aluminum plate behind them. The distance between the transmitter and the receiver is 22cm.

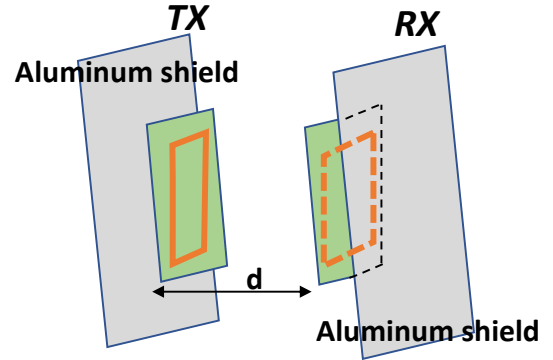


Figure 9. Link between transmitter and receiver.

4.1 Transmitting loop shape selection

To achieve higher impedance and higher magnetic flux multi-turn topology has been initially selected, but as the efficiency of the power amplifier is dependent on the parasitic losses in the antenna, we preferred to adopt a simpler single turn coil providing minimum parasitic losses. Moreover, the single turn topology allows not to take care of the self-resonance of the coil itself: this is the main reason why the multi-turn layout offers a higher parasitic resistance. The planar loop adopted for the current study is shown in the Fig. 10 (placed on a 3.5 mm-thick FR-4 substrate).

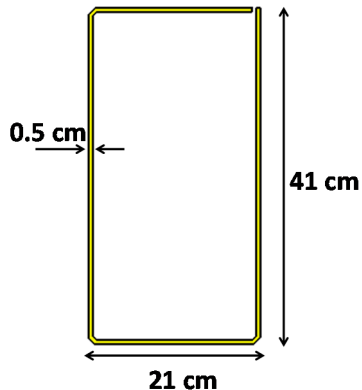


Figure 10. Transmitting coil layout.

Reducing the area of the coil would definitely reduce the parasitic resistance of the coil, but it would also decrease the magnetic flux which would lead to an inefficient power

transfer. Therefore, a tradeoff between the parasitic resistance of the coil and its area has been made after a parametric study on the coil strip width and thickness. It has been observed that, by reducing the width of the coil, we can achieve a slightly higher inductance but at the expense of an increase of the real part of the impedance; similarly, when the thickness of the coil is increased, the resistive part is slightly reduced: the reduction of few tens of $\text{m}\Omega$ is obtained for thicknesses greater than 1 mm, hence not justifying the higher cost. The final layout is shown in Fig. 11, where the copper thickness is of 70 μm : it corresponds to an $L_1=0.96 \mu\text{H}$ and a parasitic $R_1=0.36 \Omega$.

4.2 Integrated design of the inverter and the wireless link

The performance of the system has been finally evaluated for the link discussed in the previous section, being the load of the inverter. The performance for this case is shown in Fig. 11. The current waveform is still a pure sinusoid. However, there is a small degradation in the switch voltage because of the change in the loading conditions. The power delivered to the load is 2W, in this more realistic case, thus corresponding to an overall efficiency of 9%.

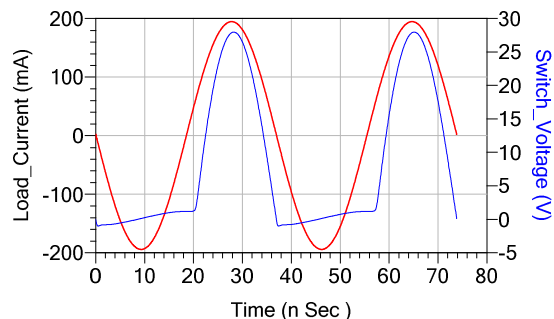


Figure 11. Voltage across switch and load current for the realistic link of Fig. 10.

5 Conclusion

A detailed investigation of a WPT link operating at 27 MHz has been carried out in this study. The unknown characteristics of the receiving coil had led to the selection of a Class E inverter as transmitting device. The need for low losses suggested to make use of a GaN transistor as switching element and to accurately design the transmitting coil. The recent acquisition of the Evaluation Board for the GS66508b transistor will allow us to test the entire system in a realistic environment.

6 References

1. C. Florian, F. Mastri, R. P. Paganelli, D. Masotti and A. Costanzo, "Theoretical and Numerical Design of a Wireless Power Transmission Link With GaN-Based Transmitter and Adaptive Receiver," in *IEEE Transactions on Microwave Theory and Techniques*, **62**, 4, April 2014, pp. 931-946, doi: 10.1109/TMTT.2014.2303949

on *Microwave Theory and Techniques*, **62**, 4, April 2014, pp. 931-946, doi: 10.1109/TMTT.2014.2303949

2. T. Nagashima, X. Wei and H. Sekiya, "Analytical design procedure for resonant inductively coupled wireless power transfer system with class-DE inverter and class-E rectifier," *2014 IEEE Asia Pacific Conference on Circuits and Systems (APCCAS)*, 2014, pp. 288-291, doi: 10.1109/APCCAS.2014.7032776
3. D. C. Marian K. Kazimierczuk, *Resonant Power Converters*, 2nd Edition, Wiley, 2011
4. R. S. Pengelly, S. M. Wood, J. W. Milligan, S. T. Sheppard and W. L. Pribble, "A Review of GaN on SiC High Electron-Mobility Power Transistors and MMICs," in *IEEE Transactions on Microwave Theory and Techniques*, **60**, 6, June 2012, pp. 1764-1783, doi: 10.1109/TMTT.2012.2187535
5. A. Pacini, F. Berra, D. Masotti and A. Costanzo, "Uniform sliding system for Simultaneous WPT and Communication Data Transfer," *2019 IEEE Radio and Wireless Symposium (RWS)*, 2019, pp. 1-3, doi: 10.1109/RWS.2019.8714337
6. A. Pacini, F. Mastri, R. Trevisan, D. Masotti and A. Costanzo, "Geometry optimization of sliding inductive links for position-independent wireless power transfer," *2016 IEEE MTT-S International Microwave Symposium (IMS)*, 2016, pp. 1-4, doi: 10.1109/MWSYM.2016.7540073
7. S. Aldhaher, P. D. Mitcheson and D. C. Yates, "Load-independent Class EF inverters for inductive wireless power transfer," *2016 IEEE Wireless Power Transfer Conference (WPTC)*, 2016, pp. 1-4, doi: 10.1109/WPTC.2016.7498864
8. S. Aldhaher, D. C. Yates and P. D. Mitcheson, "Load-Independent Class E/EF Inverters and Rectifiers for MHz-Switching Applications," in *IEEE Transactions on Power Electronics*, **33**, 10, Oct. 2018, pp. 8270-8287, doi: 10.1109/TPEL.2018.2813760